Chemical Engineering Journal 505 (2025) 159251

Contents lists available at ScienceDirect

Chemical Engineering Journal

journal homepage: www.elsevier.com/locate/cej

# A comparative life cycle assessment of Pt nanoalloy/carbon nitride/graphene electrocatalysts for PEMFC stacks

Giovanna Paladin [a], Alessandro Manzardo [b], Angeloclaudio Nale [a], Enrico Negro [a], Vito Di Noto [a,*]

[a] University of Padova, Department of Industrial Engineering, Via Marzolo 9, 35131 Padova, Italy
[b] CESQA (Quality and Environmental Research Centre), University of Padova, Department of Civil, Environmental and Architectural Engineering, Via Marzolo 9, 35131 Padova, Italy

ARTICLE INFO

*Keywords:*
Proton exchange membrane fuel cells
Life Cycle Assessment
Pt-based electrocatalysts
Graphene and related materials

ABSTRACT

The present work compares the potential environmental impact of two proton-exchange membrane fuel cell (PEMFC) stacks using life cycle assessment (LCA) methodology. The two PEMFC stacks yield the same output power, even if they have a different electrocatalyst (EC) to promote the oxygen reduction reaction (ORR). The two investigated ECs are: (i) a state-of-the-art Pt/C EC; and (ii) an innovative hierarchical $PtX_n$ nanoalloy (X = Cu and/or Ni)/Carbon Nitride/Graphene *"core–shell"* EC, labelled hereinafter *"$PtX_n$-CN/Gr"*. The latter is enabled by graphene and related materials (GRMs). The features of the PEMFC stacks in terms of functional components, operating conditions and performance are modeled on experimental results obtained from pilot devices. The contributions of the various functional components included in the PEMFC stacks (*e.g.*, the ECs, the proton-exchange membrane and the gas-diffusion layers) are quantified explicitly. The potential impact categories results are investigated through (i) a Monte Carlo analysis, to determine their uncertainties, and (ii) a sensitivity analysis, to verify their relationship with the modelling parameters (*e.g.*, the source of platinum and the scale of the synthetic process leading to the ECs). Finally, on the basis of the analysis of LCA results, a number of avenues are proposed to minimize the potential environmental impact of PEMFC systems.

## 1. Introduction

The transport sector accounts for approximately 25 % of today's Europe's greenhouse gas (GHG) emissions [1]. As a result, this sector was identified as a key area for action of the European Green Deal, a set of policy initiatives with the main goals of reaching by 2050 a state of net zero carbon and decoupling economic growth from resource use. According to European strategy, to foster the development and large-scale rollout of zero- and low- emission vehicles is crucial. A promising option is identified in hydrogen fuel cell vehicles, with a particular reference to *"heavy-duty"* systems such as trucks, boats and trains as suitable for long-distance transportation and for which several investments are supported under the EU energy system integration and hydrogen strategies [2].

Proton exchange membrane fuel cells (PEMFCs) fed on direct hydrogen are the most promising fuel cell systems to power vehicles due to: (i) a high energy conversion efficiency; (ii) a high power density; (iii) a sufficient durability; and (iv) very fast start/stop features. However, several problems need to be addressed to achieve a widespread application of this technology in the market. Hydrogen supply is an issue mainly due to costs regarding both fuel price itself and requirements of a suitable and widespread infrastructure. Hydrogen safety is also an issue, as hydrogen storage raises concerns both in terms of risk assessment and of social acceptability [3].

An important shortcoming that significantly constrains the energy conversion efficiency of PEMFCs is the sluggish kinetics of the oxygen reduction reaction (ORR) taking place at the cathode electrode. The ORR needs to be promoted by an effective electrocatalyst (EC) to ensure that the PEMFC exhibits a performance and a durability level complying with the requirements of applications. The conventional ORR ECs for state-of-the-art PEMFCs consist of Pt nanoparticles supported on carbon [4]. Such ECs, which are usually indicated as *"Pt/C"* ECs, allow for the fabrication of PEMFCs exhibiting a good level of performance and a sufficient durability. The abundance of platinum in Earth's crust is very

* Corresponding author.
*E-mail addresses:* giovanna.paladin@unipd.it (G. Paladin), alessandro.manzardo@unipd.it (A. Manzardo), angeloclaudio.nale@unipd.it (A. Nale), enrico.negro@unipd.it (E. Negro), vito.dinoto@unipd.it (V. Di Noto).

https://doi.org/10.1016/j.cej.2025.159251
Received 22 July 2024; Received in revised form 21 December 2024; Accepted 2 January 2025
Available online 3 January 2025

limited. Indeed, Pt is present on the list of critical raw materials proposed by the European Union [5]. Thus, major efforts are currently underway to minimize the amount of Pt in the ECs of PEMFCs without compromising performance and durability.

Several approaches were proposed to address the performance and durability shortcomings of state-of-the-art ECs both in relation to the chemical composition of the active sites (*e.g.*, by the implementation of alloys between platinum and other metals, which boost the electrochemical kinetics) and with respect to the support, where both carbon and non-carbon carriers alternatives were proposed [6]. As regards the support, carbon black offers several benefits due to its simple preparation, high conductivity (that minimizes ohmic losses) and low cost. On the other hand, carbon black suffers from stability and corrosion issues when exposed to a high electrochemical potential in oxidizing conditions (*e.g.*, at the cathode of PEMFCs). These drawbacks are mostly caused by: (i) defects in the graphite lattice, which may trigger the detachment of Pt active sites upon PEMFC operation; and (ii) weak interactions between the Pt active sites and the support as a consequence of common preparation methods of Pt/C ECs, facilitating the growth, agglomeration or detachment of Pt nanoparticles with the consequent loss of active area. Several solutions were proposed in the literature to improve the durability of ECs for PEMFCs, such as different synthesis methods to inhibit the growth of Pt nanoparticles or the development of highly graphitized supports to minimize EC corrosion [7].

A breakthrough synthetic route was devised over the course of the last 15 years to address the performance and durability shortcomings of state-of-the-art Pt/C ECs for PEMFCs [8–12]. Such route yields ORR ECs wherein a *"core"* support (typically consisting of more than one carbon species) is coated by a carbon nitride (CN) *"shell"* with a concentration of N atoms lower than 5 wt% coordinating plurimetallic nanoparticles bearing the active sites [8]. This synthetic route is extremely flexible and allows to tailor crucial features of the final ORR EC such as the chemical composition of the active sites and the morphology [8]. The adoption of active sites combining Pt (acting as the *"catalyst"*) and one or more first-row transition elements such as Ni and Cu (the *"co-catalysts"*) improves by up to one order of magnitude the intrinsic EC kinetics of pure Pt in the ORR [8], allowing to drastically reduce the loading of precious metals on the PEMFC cathode. The strong chemical interactions established between the plurimetallic nanoparticles bearing the ORR active sites and the CN *"shell"* enhance the EC durability [8]. Finally, the adoption of suitable hierarchical carbonaceous *"cores"* yields ECs exhibiting simultaneously: (i) an excellent conductivity, minimizing ohmic losses, and (ii) a morphology allowing for the facile transport of reactant and products, enabling the achievement of high current densities [8].

Graphene and related materials (GRM) exhibit a very high electrical conductivity and their 2D features promote mass transport [11]. On these bases, GRMs were proven to be highly promising for implementation in the support of hierarchical *"core–shell"* CN ECs for the ORR [8,11]. The development of GRM-enabled hierarchical *"core–shell"* CN ECs for the ORR was carried out mostly in the framework of the Graphene Flagship, a major undertaking of the European Union meant to bring to the market applications and products based on GRMs [13]. One of the GRM-enabled hierarchical *"core–shell"* CN EC for the ORR devised in the Flagship is indicated as *"$PtX_n$-CN/Gr"*. In such EC, *"$PtX_n$"* alloy nanoparticles (X = Cu and/or Ni) bearing the active sites are coordinated on a CN *"shell"* covering a GRM-enabled support *"Gr"*. With respect to the conventional synthetic routes adopted to obtain state-of-the-art Pt/C ECs, the approach pursued to prepare $PtX_n$-CN/Gr is completely different as it involves different reactants and innovative processes at high temperature (up to T = 900 °C) [8–11,14,15].

The purpose of this study is to verify the potential environmental feasibility to implement the GRM-enabled hierarchical $PtX_n$-CN/Gr ORR EC in the fabrication of a PEMFC stack (labelled hereinafter as *"I-stack"*), adopting as the reference a state-of-the-art PEMFC stack, (labelled hereinafter as *"R-stack"*) yielding the same output power and mounting a conventional ORR Pt/C EC. A particular focus is dedicated: (i) to present the contribution of the various functional components included in the system (*e.g.*, electrocatalysts – ECs, proton-exchange membranes – PEMs, gas-diffusion layers – GDLs); and (ii) to develop a framework able to comprehensively quantify the potential environmental impacts of the proposed ORR EC for PEMFCs in a highly fragmented scientific panorama characterized by important discrepancies between different studies [16]. Indeed, though state-of-the-art fuel cell vehicles (*e.g.*, the Toyota Mirai) mount special cathodic ECs comprising Pt-M alloys (see for instance the following URL: [17]), the latter are not commonly/easily available on the open market for research purposes. In addition, the steps involved in the preparation of such special cathodic electrocatalysts are not in the public domain. Thus, the introduction of such special cathodic electrocatalysts in the LCA would have jeopardized the latter's accuracy. For all these reasons, it was decided to benchmark the features of the *"I-stack"* (mounting the innovative hierarchical GRM-enabled $PtX_n$-CN/Gr EC) with a *"R-stack"* only including conventional and well-known Pt/C reference ECs.

## 2. Methods and strategies

The potential environmental impacts of the PEMFC stacks described in this work are obtained by means of the Life Cycle Assessment (LCA) methodology, whose main phases are briefly outlined hereinafter in Section 2.1.1. – Section 2.1.3. Subsequently, the synthetic approach pursued to obtain the GRM-enabled hierarchical $PtX_n$-CN/Gr ORR EC is presented (see Section 2.2). Finally, it is described the methodology to implement $PtX_n$-CN/Gr and a conventional Pt/C ORR EC into single PEMFCs, that are tested in operating conditions to obtain the performance figures on the basis of the analysis of the potential environmental impacts (see Section 2.3).

### 2.1. Life cycle assessment (LCA)

The Life Cycle Assessment (LCA) methodology is applied to perform the comparison between the potential environmental impacts of the *"I-stack"* and the *"R-stack"* considered in this work. LCA is the most suitable methodology to pursue this goal since it is: (i) broadly recognized; (ii) standardized; and (iii) transparent and rigorous. In addition, the application of LCA allows a comprehensive overview of the different categories of potential environmental impact and support informed decision to reduce them. According to the standards (ISO 14040 2006) and (ISO 14044 2006), LCA is organized into four phases: (i) goal and scope definition (see Section 2.1.1.); (ii) inventory analysis (see Section 2.1.2.); (iii) impact assessment; and (iv) interpretation. The modelling and assumptions for impact assessment and interpretation are provided in Section 2.1.3.

#### 2.1.1. Goal and scope definition

The main goal of this study is to compare the potential environmental impact of the *"I-stack"* and the *"R-stack"*, following the general guidelines reported in the literature [18]. The two devices have the same function defined as the delivery of an output power of 80 kW powering a *"light-duty"* vehicle [19]. Table 1 reports the main features of the stacks considered including components, operating conditions and performances. The platinum loading and the geometric area of the PEMFC electrodes mimic the figures of the state of the art [19,20]. The operating conditions and the performance of the PEMFC stacks reported in Table 1 are experimental data obtained as described in Section 2.3.

The number of membrane-electrode assemblies (MEAs) mounted in each PEMFC stack is set so that the latter yields the chosen output power. The main difference between the two PEMFC stacks is that the overall mass of EC used in the *"I-stack"* is lower compared to the mass in the *"R-Stack"* (36.7 g, including 14.7 g of Pt *vs*. 60.9 g, including 24.4 g of Pt). It is highlighted that the $PtX_n$-CN/Gr EC is best run with feeds exhibiting a pressure of 4–5 bar [8,15]. On the other hand, the conventional *"state-of-the-art"* PEMFC stacks for *"light-duty"* vehicles are typically operated

**Table 1**
Main features of the analyzed PEMFC stacks.

| *Features of the electrodes* | | | | |
|---|---|---|---|---|
| PEMFC stack | *"I-stack"* | | *"R-stack"* | |
| *Electrode* | Anode | Cathode | Anode | Cathode |
| *EC* | Pt/C | $PtX_n$-CN/Gr | Pt/C | Pt/C |
| *wt% of Pt in the EC* | 40 | 40 | 40 | 40 |
| *Pt loading/mg$_{Pt}$•cm$^{-2}$* | 0.05 | 0.10 | 0.05 | 0.30 |
| *EC loading/mg•cm$^{-2}$* | 0.125 | 0.25 | 0.125 | 0.75 |
| *Geometric area/cm$^2$* | 267 | 267 | 267 | 267 |
| *EC mass on a single membrane-electrode assembly (MEA)/mg* | 33.375 | 66.75 | 33.375 | 200.25 |

| ***Other features*** | | |
|---|---|---|
| **PEMFC stack** | ***"I-stack"*** | ***"R-stack"*** |
| *Total loading of Pt on a single MEA/ mg$_{Pt}$•cm$^{-2}$* | 0.15 | 0.35 |
| *Operating pressure/bar* | 4–5 | 2 |
| *Geometric power density/W•cm$^{-2}$* | 0.986 | 1.15 |
| *Specific power/kW•g$_{Pt}^{-1}$* | 6.57 | 3.29 |
| *Output power of the single MEA/W* | 263 | 307 |
| *Number of MEAs in the PEMFC stack* | 304 + 57[a] | 261 |
| *Total mass of EC in the PEMFC stack/g* | 10.14[b] + 2.10[a]<br>20.28[c] + 4.19[a] | 8.70[b]<br>52.17[c] |
| *Total mass of Pt in the PEMFC stack/g* | 14.7[d] | 24.4 |
| *Output power of the PEMFC stack/kW* | 80 | 80 |

[a] This adjustment accounts for the fact that the *"I-stack"* operates at a higher pressure in comparison with the *"R-stack"*. Additional details are provided in Section 2.1.1.
[b] On all the anode electrodes of the PEMFC stack.
[c] On all the cathode electrodes of the PEMFC stack.
[d] This value includes the additional EC to account for the higher operating pressure.

at a lower pressure, on the order of 2 bar [21]. This discrepancy is justified considering that, with respect to the GRM-enabled $PtX_n$-CN/Gr EC, the conventional Pt/C EC mounted in the *"R-stack"* exhibits much weaker interactions between the support and the Pt nanoparticles bearing the active sites [8]. Hence, if a conventional Pt/C EC is operated at 4–5 bar it would not exhibit a sufficient durability for the intended application in a *"light-duty vehicle"*. This issue is an important shortcoming of conventional Pt/C ECs; indeed, massive efforts are currently underway to devise next-generation ECs suitable for operation in *"heavy-duty"* vehicles (*e.g.*, trucks) at a higher pressure of the feeds and achieving a much improved durability [22]. In this work, for the sake of simplicity, it is assumed that the *"I-stack"* and the *"R-stack"* exhibit the same durability. This assumption is reasonable if we consider that, with respect to the conventional Pt/C EC, the $PtX_n$-CN/Gr EC is characterized by at least the same tolerance to accelerated ageing in *"ex-situ"* tests (data not shown). With respect to operation at a pressure of 2 bar, operation at a pressure of 4–5 bar can only be achieved by investing a higher share of the output power of the PEMFC stack (*e.g.*, to run a compressor). To account for this issue, the number of MEAs in the *"I-stack"* modeled in Table 1 is increased by *ca.* 20.6 % to ensure that the total *"net"* output power was 80 kW. In other words, for the LCA analysis, to compare the two systems using the same functional unit (*i.e.*, a net power output of 80 kW), a gross power of approximately 95 kW was considered for the *"I-stack"* system. This adjustment takes into account the additional power required to compensate for the increased air compression needed in this configuration. Fig. 1 displays the general framework of boundaries of the investigated systems.

In Fig. 1(a) and (b) it is shown that a PEMFC stack consists of a series of MEAs, each sandwiched between two bipolar plates. The PEMFC stack is completed by two additional end plates. Each MEA consists of: (i) one proton-exchange membrane (PEM); (ii) two electrocatalytic layers (EC layers) in direct contact with the PEM; (iii) two gas diffusion layers (GDLs), each covering one EC layer; and (iv) two sub-gaskets. System boundaries are set *"from cradle to gate"*, from raw materials extraction to the production of the MEAs and of the bipolar plates. End plates are not covered in the present analysis to minimize the extension of the modeled system. For the sake of comparison, only the components that are different in the two PEMFC stacks under investigation are considered. The analysis carried out in this work covers the required and the recommended impact categories lists outlined in conventional guidelines [18] and presented in Table 2. Some impact categories (*e.g.*, human toxicity and ecotoxicity) are considered herein to ensure comprehensiveness, even if they present a lack of solid data and research on related characterization models (*e.g.*, the research on the impacts of nanoparticles on metabolism and others is still ongoing) [23].

The PEM, GDLs, sub-gaskets, MEA assembly process and bipolar plates are modelled in accordance with a highly regarded PEMFC systems cost projection study found in the open literature [20]. This is characterized by a continuous improvement of the data and of the comparison with market solutions. Missing information is integrated from patents and other literature sources [24–30]. The models for the production of the Pt/C EC and the $PtX_n$-CN/Gr EC at the commercial extent are obtained by upscaling the laboratory procedures described in Section 2.3. The energy expenditure for the synthesis is modelled according to a framework described in the literature, *i.e.*, considering minimum energy requirements and proxy values [31]. The assumed efficiencies of the various processes involving the ECs considered in this report are shown in Table 3. The production efficiency of the GRM-enabled hierarchical $PtX_n$-CN/Gr EC is estimated on the basis of the evaluations of experts. The evaluation of the production efficiency of the Pt/C EC and of the platinum recycling process is based on literature [20]. The process efficiencies reported in Table 3 model a production at the industrial scale. The treatment of wastes is handled according to a general approach [32], *i.e.*, considering wastewater treatment for aqueous wastes and waste incineration for organic wastes. Air emission treatment is considered when a proper dataset is available. Finally, it is assumed that the platinum used in the synthesis of the ECs considered in this paper is obtained from primary sources.

### 2.1.2. Inventory analysis

The LCA study of a chemical process is typically very challenging due to: (i) the large amount of data needed; and (ii) the limited availability of publicly available datasets for the chemicals. This is especially true for LCA studies of new processes and technologies, where a broad variety of solutions are available for each component. Several approaches exist for the characterization of chemicals and chemical processes [33]. Some approaches exhibit a higher accuracy (*e.g.*, those exploiting plant data or implementing a process simulator) [34]; some other approaches require fewer data (*e.g.*, those relying on process calculations, stoichiometry, molecular structured models, or using a proxy). The latter is applicable when there is accessible data for a similar compound, by means of a substance with similar properties and well-described in LCA databases, the potential environmental impact of an unknown substance can be reasonably estimated. In this report, most information is retrieved from the Ecoinvent 3.8 databases [34]. Publications and patents are exploited to fill the gaps of the Ecoinvent 3.8 databases on specific substances, materials and laboratory methodologies. With reference to energy and material flows, for which only synthesis information was available, they were estimated starting from laboratory data. The energy and the amounts are estimated through the literature [31]. In the case no information were available, similar substances having the same function were used as proxy data. In particular, the framework proposed in the literature [31] is adopted to the processes for the synthesis of both the Pt/C EC and the $PtX_n$-CN/Gr EC. Accordingly, in this study the methodological approach and the data assumptions are aligned for the two technologies under study, yielding a harmonized inventory.

The inventory for the $PtX_n$-CN/Gr EC is assembled in accordance with the preparation procedure described in Section 2.2 and is detailed in Table 1 of Supplementary Materials. The process reactants unavailable in the Ecoinvent 3.8 databases are modelled based on information

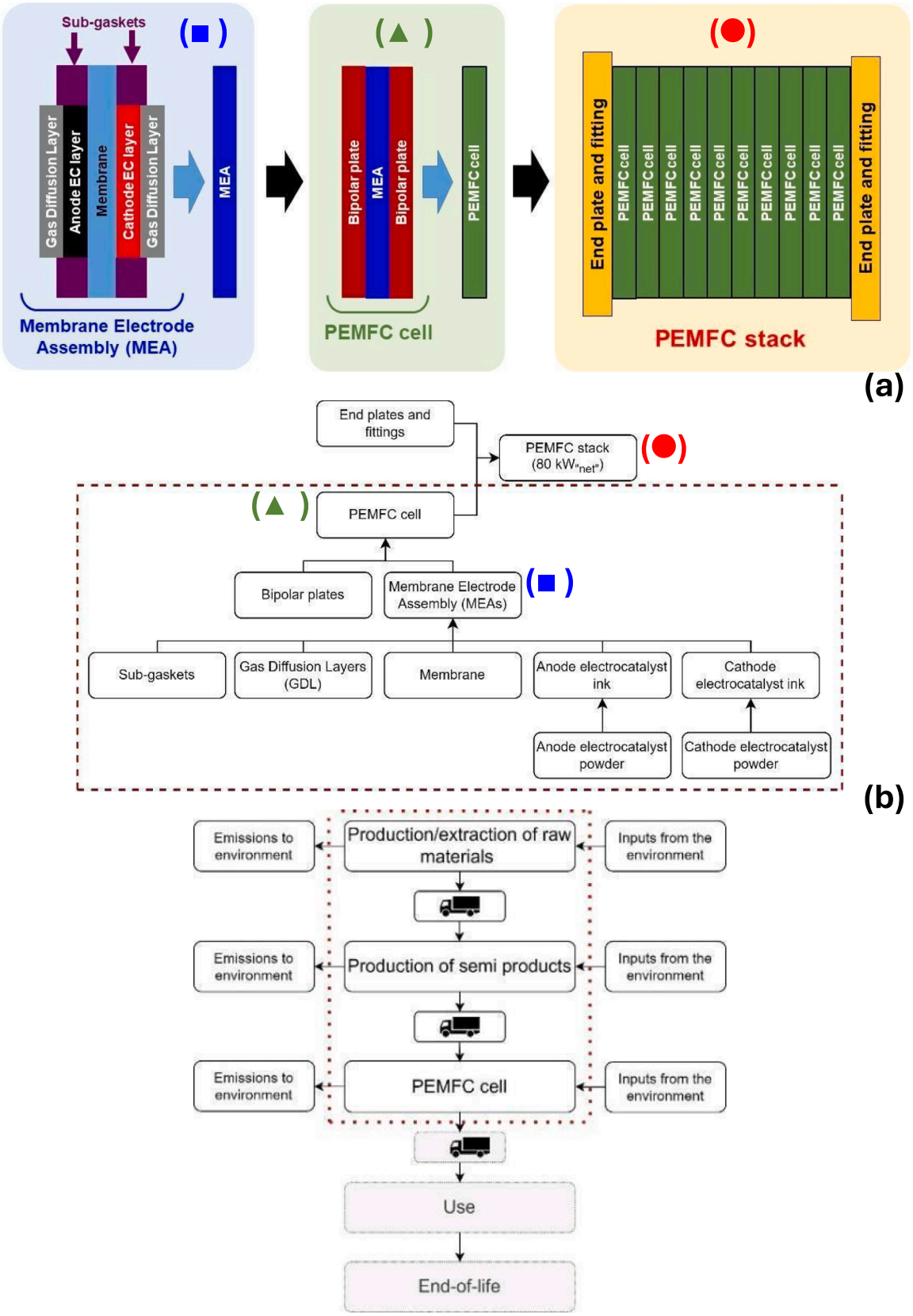


**Fig. 1.** (a) Scheme of a PEMFC stack. (b) System boundaries general framework.

**Table 2**
Impact categories under consideration and selected characterization models.

| Impact category | Characterization model | Units |
|---|---|---|
| *Global Warming Potential* | Baseline model of 100 years of the IPCC, from EF method version 3.0 (JRC Technical Reports 2018) | kg $CO_2$ eq. |
| *Acidification Potential* | Accumulated Exceedance, from EF method version 3.0 (JRC Technical Reports 2018) | kg $SO_2$ eq. |
| *Eutrophication Potential* | Accumulated Exceedance, from EF method version 3.0 (JRC Technical Reports 2018) | kg $PO_4^{3-}$ eq. |
| *Abiotic depletion, elements* | CML Guinée *et al.* (2002) and van Oers *et al.* (2002), from EF method version 3.0 (JRC Technical Reports 2018) | kg Sb eq. |
| *Abiotic depletion, fossil fuels* | CML Guinée *et al.* (2002) and van Oers *et al.* (2002), from EF method version 3.0 (JRC Technical Reports 2018) | MJ |
| *Non-renewable Primary Energy Demand* | Non-renewable from Cumulative Energy Demand (Hans-Jörg Althaus 2010) | MJ |
| *Renewable Primary Energy Demand* | Renewable from Cumulative Energy Demand (Hans-Jörg Althaus 2010) | MJ |
| *Ozone depletion potential* | Steady-state ODP, from EF method version 3.0 (JRC Technical Reports 2018) | kg $CFC^{-11}$ eq. |
| *Respiratory inorganics* | PM method recommended by UNEP, from EF method version 3.0 (JRC Technical Reports 2018) | disease incidences |
| *Ionising radiation* | Human health effect model as developed by Dreicer et al. 1995, from EF method version 3.0 (JRC Technical Reports 2018) | kBq $U^{-235}$ eq. |
| *Photochemical ozone formation potential* | LOTOS-EUROS, from EF method version 3.0 (JRC Technical Reports 2018) | kg NMVOC eq. |
| *Land use* | Soil quality index based on LANCA, from EF method version 3.0 (JRC Technical Reports 2018) | Pt |
| *Human Toxicity* | USEtox model based on USEtox 2.1 model (Fantke et al. 2017), adapted as in Saouter et al., 2018 | kg 1,4-DB eq. |
| *Freshwater aquatic ecotoxicity* | USEtox model based on USEtox 2.1 model (Fantke et al. 2017), adapted as in Saouter et al., 2018 | kg 1,4-DB eq. |
| *Marine aquatic ecotoxicity* | USEtox model based on USEtox 2.1 model (Fantke et al. 2017), adapted as in Saouter et al., 2018 | kg 1,4-DB eq. |
| *Terrestrial ecotoxicity* | USEtox model based on USEtox 2.1 model (Fantke et al. 2017), adapted as in Saouter et al., 2018 | kg 1,4-DB eq. |

**Table 3**
Assumptions on process efficiencies.

| Processes | Process efficiency |
|---|---|
| *Synthesis of the Pt/C EC* | 95 % |
| *Synthesis of the GRM-enabled support for $PtX_n$-CN/Gr* | 95 % |
| *Synthesis of $PtX_n$-CN/Gr* | 85 % |
| *Post-processing of $PtX_n$-CN/Gr* | 95 % |
| *Platinum recycling process* | 94 % |

retrieved in the literature, as described in the following chapters. Graphene nanoplatelets are modelled considering the reduction of graphene oxide by hydrazine monohydrate [35,36]. It is assumed that primary $K_2PtCl_4$ is synthesized starting from $H_2PtCl_6$ following the procedure described in the literature [28]. Recycled platinum is modelled based on the information reported in the literature [37]. $K_2Ni(CN)_4{\cdot}nH_2O$ is described following the procedure reported in the literature [38]. Finally, it is assumed that Cu nanoparticles are obtained by reducing copper nitrate with hydrazine monohydrate using Ag nanoparticles as the catalyst [25].

The inventory for the Pt/C EC mounted at: (i) the anode of both the PEMFC stacks; and (ii) the cathode of the *"R-stack"* (see Table 1) is presented in Table 2 of Supplementary Materials. The inventory for the Pt/C EC is built based on the literature [24]. It is assumed that: (i) formaldehyde is used as the reducing agent; and (ii) the process efficiency is equal to 95 % (see Table 3). The study above implements a general method for the synthesis of Pt/C ECs based on impregnation/reduction in a liquid phase using a slurry tank mounting a pH and a temperature controller and using formaldehyde as the reducing agent [30].

The inventory for the proton-exchange membrane (PEM) used in all the MEAs mounted in the PEMFC stacks considered in this work is reported in Table 3 of Supplementary Materials. The PEM is characterized by a thickness of 14 μm and consists of Nafion® reinforced by an ePTFE support. The PEM is synthesized by means of two individual coating and drying steps [20]; specifically, a first Nafion layer reinforced by ePTFE is formed on top of a second protective Nafion layer. The composition of the Nafion dispersion that is dried to obtain the first Nafion layer reinforced with ePTFE is the following: Nafion – 5 wt%; isopropanol – 47.5 wt%; methanol: 47.5 wt%. The composition of the Nafion dispersion that is dried to obtain the second Nafion layer is the following: Nafion – 5 wt%; water – 90 wt%; hexanol – 3 wt%; isopropanol – 2 wt% [20]. The yield of ePTFE and Nafion are assumed to be equal to 95 % and 94 %, respectively. Nafion is modeled in accordance with the literature [39].

The formulation of the electrocatalytic inks is the following: 15 wt% of dry EC powder; 37.5 wt% methanol; 37 wt% distilled water and 10 wt % of Nafion [20]. Each electrocatalytic ink is homogenized by ultrasonication for 48 h [40] and then deposited onto the PEM, yielding the *"catalyst-coated membrane"* (CCM). The inventory for the CCM mounting at the cathode either the *"innovative"* GRM-enabled hierarchical $PtX_n$-CN/Gr EC or the conventional Pt/C EC is reported respectively on Table 4 and Table 5 of Supplementary Materials.

All the MEAs considered in this work mount the same GDLs on both

**Table 4**
Outcomes of life cycle impact assessment on the environmental impact of 80 kW PEMFC stacks considered in this work.

| Impact category | Unit | *"I-stack"* | *"R-stack"* | Difference/ % |
|---|---|---|---|---|
| *Global warming (GWP100a)* | kg $CO_2$ eq. | 1.53E + 03 | 2.11E + 03 | −27 |
| *Acidification* | kg $SO_2$ eq. | 6.83E + 01 | 1.10E + 02 | −38 |
| *Eutrophication* | kg $PO_4^{3-}$ eq. | 8.22E + 00 | 1.25E + 01 | −34 |
| *Abiotic depletion, elements* | kg Sb eq. | 6.03E-02 | 9.58E-02 | −37 |
| *Abiotic depletion, fossil fuels* | MJ | 2.07E + 04 | 2.96E + 04 | −30 |
| *Non-Renewable Primary Energy Demand* | MJ | 2.33E + 04 | 3.22E + 04 | −28 |
| *Renewable Primary Energy Demand* | MJ | 1.21E + 03 | 1.27E + 03 | −5 |
| *Ozone layer depletion (ODP)* | kg $CFC^{-11}$ eq. | 9.45E-04 | 7.84E-04 | +21 |
| *Ionising radiation* | kBq $U^{-235}$ eq. | 1.67E + 02 | 1.79E + 02 | −7 |
| *Photochemical ozone formation* | kg NMVOC eq. | 2.42E + 01 | 3.82E + 01 | −37 |
| *Particulate matter* | disease inc. | 2.46E-04 | 3.83E-04 | −36 |
| *Land use* | Pt | 1.20E + 04 | 1.78E + 04 | –33 |
| *Human Toxicity* | kg 1,4-DB eq. | 3.25E + 02 | 4.21E + 02 | −30 |
| *Freshwater aquatic ecotoxicity* | kg 1,4-DB eq. | 4.74E + 00 | 3.75E + 00 | +20 |
| *Marine aquatic ecotoxicity* | kg 1,4-DB eq. | 1.28E + 06 | 1.85E + 06 | −44 |
| *Terrestrial ecotoxicity* | kg 1,4-DB eq. | 1.39E + 00 | 9.67E-01 | +30 |

**Note:** *"I-stack"* refers to the stack fabricated using the GRM-enabled hierarchical $PtX_n$ -CN/Gr ORR EC for a PEMFC. The *"R-stack"* refers to a reference stack, which represents the current state-of-the-art PEMFC stack and is used for comparison. Difference/% = [(I-stack–R-stack)/R-stack]•100.

electrodes. The inventory of such GDLs is displayed in Table 6 of Supplementary Materials. Each GDL is made of a carbon paper with a macroporous structure (MPS) and a microporous layer (MPL). The thickness of the MPS and of the MPL is equal to 105 and 45 μm, respectively [20]. The manufacturing of GDLs consists of three steps: (i) fabrication of the carbon fiber paper; (ii) treatment of the carbon fiber paper by a phenolic resin followed by a PTFE treatment to ensure hydrophobicity; and (iii) application of the MPL by ink coating followed by sintering.

The MEAs considered in this study include sub-gaskets. Each sub-gasket consists of a polyethylene terephthalate (PET) film with a thickness of 100 μm. One sub-gasket is applied by means of a roll-to-roll process on each side of the MEA, covering 1/8 of the PEM [20]. The inventory of each complete MEA is shown in Table 7 of Supplementary Materials.

The bipolar plates included in both the PEMFC stacks considered in this work are made of stainless steel and are obtained starting from a sheet of metal with a thickness of 76.2 μm and applying a press force of 10000 kN per stroke [20]. The edges of each bipolar plate are laser-welded to avoid the need for a separate coolant gasket. The inventory for each bipolar plate is reported on Table 8 of Supplementary Materials.

#### 2.1.3. Modelling and assumptions for impact assessment and interpretation

The classification of elementary flows and characterization of potential environmental impacts are carried out using the software SimaPro 9.4.0.2. [41]. The assessment considers explicitly the various contributions provided by: (i) the components of the PEMFC stacks (*e.g.*, ECs, the PEM, GDLs, sub-gaskets and bipolar plates); and (ii) other aspects such as the assembly and transport. A base case scenario is assessed considering a mean value for each parameter involved.

In a subsequent step, uncertainty analysis was performed through Monte Carlo analysis [42]. Accordingly, the characterizing flows of the two systems under comparison are perturbed randomly within the respective ranges of uncertainty for a total of 1000 iterations. The results provide uncertainty of each impact category results. The analysis is carried out simultaneously for the two systems under comparison. Consequently, the same perturbation is applied to the flows of both systems. Three sensitivity analysis of the base case scenario are performed to investigate how different decisions and assumptions affected the relative contributions of each unit process to the potential impact category results.

The first sensitivity, referred hereafter as Sensitivity 1, investigates the supply chain of platinum if 60 % of the platinum used in the synthesis of all the ECs is obtained from the end-of-life recovery of automotive catalytic converters. In 2022 the total gross demand of platinum was *ca.* 193 tons [43]. 40 % of this demand, *ca.* 77 tons, was from the automotive industry. In 2022 the amount of platinum obtained from recycling was estimated to be *ca.* 46 tons, of which 75 % came from the automotive sector. Thus, *ca.* 35 tons of platinum were recycled from the automotive sector in 2022. In conclusion, in 2022 *ca.* 45 % of the demand of platinum from the automotive sector was covered by platinum recycled from the automotive sector itself. This latter figure is in line with statistics of previous years [44]. It is estimated that the market rollout of the various families of fuel cell vehicles will increase the overall demand of platinum by a factor between 3x and 10x [45]. It is very optimistic to assume that 60 % of platinum could be obtained from recycling. Nevertheless, this figure is considered for the specific purpose to model the effects on the assessment carried out in the present study originating from a significant decrease in the prevalence of platinum obtained from primary sources (*i.e.*, mining). This scenario is also consistent with the strong emphasis placed both in the European Union and at the global level to maximize the recycling of strategic elements (which include platinum) [46]. It is highlighted that the state-of-the-art approaches to recycle platinum from the electrodes of *"spent"* PEMFCs, which typically involve leaching in suitable combinations of acids and/or oxidizing agents [47], are expected to be equally effective on both the PEMFC stacks considered in this work. The latter include the *"R-stack"*, only comprising a conventional Pt/C EC, and the *"I-stack"*, mounting the $PtX_n$-CN/Gr EC. This is because: (i) the latter EC only includes first-row transition metal *"co-catalysts"* [8] (*i.e.*, Ni and Cu, see Section 1), which are less chemically stable than Pt and do not hinder its extraction; and (ii) the leaching processes are designed to operate effectively on the anode electrodes, whose platinum loading is lower than that of the cathode electrodes (see Table 1). Correspondingly, Pt recycling is not expected to influence negatively the feasibility of $PtX_n$-CN/Gr EC for practical applications.

The second sensitivity, also referred as Sensitivity 2, address the modelling of the Nafion proton-exchange ionomer. Indeed, literature provides little information to allow a complete modelling of Nafion. In this study a conservative approach is used for the reference scenario [39]. The sensitivity analysis considers an alternative modelling of Nafion proposed in [48]. This latter takes into consideration the only database currently available for Nafion [49] and reports the potential environmental impact of Nafion for several impact categories, nevertheless, results related to primary energy demand are not included as they are not documented in the literature.

A third sensitivity, referred hereafter as Sensitivity 3, investigate the production of ECs assuming that they are produced at laboratory scale, wherein in the base case scenario it is assumed that the ECs are produced at industrial scale (see Section 2.1.1.). At the laboratory scale: (i) the recycling of platinum is not considered; (ii) the efficiency in the production of both Pt/C EC and $PtX_n$-CN/Gr EC is set to 70 %; (iii) the efficiency in the post-processing of $PtX_n$-CN/Gr is set to 90 %; and (iv) the energy consumption of the laboratory equipment involved in the EC production is estimated to be 30 % of the average energy requirement. The efficiencies in (ii) and (iii) are consistent with typical values registered during the preparation of the $PtX_n$-CN/Gr EC at the laboratory scale by the authors.

### 2.2. Preparation of the GRM-enabled hierarchical $PtX_n$-CN/Gr EC

The GRM-enabled hierarchical $PtX_n$–CN/Gr EC is synthesized following a proprietary procedure that is described in the technical literature [9,50]. This procedure includes three main steps and is briefly outlined in the following.

*Graphene pre-treatment.* Graphene nanoplatelets (2–10 nm, ACS Material®) are progressively added to ZnO nanoparticles (d = 40–100 nm, Alfa Aesar) up to a 1:4 mass proportion. The mixture is extensively ball milled. The resulting powders are then: (i) treated with a 5 wt% HCl solution for 1 h; (ii) washed with doubly distilled water until neutrality; and (iii) dried at 100 °C for 4 h, yielding the *"pre-treated graphene"*.

*Precursor synthesis and activation.* A first dispersion is prepared, including: doubly distilled water; $K_2PtCl_4$ (99.9 %, ABCR); Cu nanoparticles (99.9 %, 25 nm, IoLiTec nanomaterials); sucrose (99+%, Acros); and equal amounts of Vulcan® XC-72R carbon black (Cabot) and the *"pre-treated graphene"* described above. The dispersion is homogenized by: (i) stirring for 1 h; and (ii) probe sonication for 5 min. A second dispersion is prepared, that is identical to the first dispersion just described above, with the only difference that $K_2Ni(CN)_4{\cdot}xH_2O$ (98 %, Sigma-Aldrich) is used instead of $K_2PtCl_4$. This second dispersion is homogenized exactly as described above. The first dispersion is added dropwise into the second dispersion. The resulting product undergoes probe sonication for 2 min and stirring for 16 h before being allowed to rest for 48 h. The product is dried at 120 °C and then transferred into a quartz tube furnace, wherein the following multi-step heat treatment is carried out under a dynamic vacuum ($10^{-2}$ mbar, obtained by a rotary pump): 2 h @ 150 °C; 2 h @ 300 °C and 2 h @ 600 °C. The resulting product is treated in 2 M $H_2SO_4$ under stirring at 70 °C for 24 h, washed with doubly distilled water until neutrality and finally dried, yielding the *"rough electrocatalyst"*.

*Post-processing.* The *"rough electrocatalyst"* is progressively added to ZnO nanoparticles (d = 40–100 nm, Alfa Aesar) up to a 1:3 mass

proportion. The mixture is ball milled for 5 min. The resulting powders are then: (i) treated with 0.5 M $HNO_3$ for 20 min; (ii) washed with doubly distilled water until neutrality; and (iii) dried at 100 °C for 4 h, yielding the final disaggregated $PtX_n$-CN/Gr EC. The latter includes 39.8 wt% of Pt, 1.2 wt% of Ni and 3.6 wt% of Cu, as determined by inductively-coupled plasma atomic emission spectroscopy (ICP-AES).

### 2.3. Fabrication of membrane-electrode assemblies (MEAs) and testing in single-cell configuration

15 mg of HiSPEC™ 4000Pt/C EC (40 wt% of Pt, Johnson Matthey fuel Cells) are suspended into 75 mg of a 1:1 wt/wt solution of water and isopropyl alcohol. Subsequently, 215 μL of a Nafion® D-521 dispersion (Sigma-Aldrich) are added; the resulting mixture undergoes probe sonication for 5 min and is then brought to *ca.* 50 °C under stirring. The solvent is allowed to evaporate under stirring until the final homogenized EC ink weighs 100 mg. The ink is blade-coated onto a GORE-SELECT® membrane M775, achieving a Pt loading of 0.05 mg•cm$^{-2}$. The resulting EC layer is a square whose side is 2 cm long. Afterwards, the same EC ink is blade-coated onto the same area on the opposite side of the membrane. A square EC layer whose side is 2 cm long and including a Pt loading of 0.3 mg•cm$^{-2}$ is obtained, resulting in a CCM. Two 2.1 x 2.1 cm pieces of Sigracet™ 22BC carbon paper are then hot-pressed on the EC layers deposited on the CCM, yielding the final membrane-electrode assembly (MEA). The latter comprises the HiSPEC 4000Pt/C EC (indicated hereinafter as *"Pt/C reference"*) on both the anode (Pt loading: 0.05 mg•cm$^{-2}$) and the cathode (Pt loading: 0.3 mg•cm$^{-2}$).

A second MEA is prepared, that is exactly identical to the one described above, with the only difference that the cathodic EC layer includes the disaggregated GRM-enabled hierarchical $PtX_n$-CN/Gr EC. The Pt loading in the $PtX_n$-CN/Gr EC is 40 wt%. The ink comprising the $PtX_n$-CN/Gr EC is prepared exactly as described above for the ink including the HiSPEC™ 4000Pt/C EC; the only difference is that the ink includes 15 mg of $PtX_n$-CN/Gr EC. All the remaining steps involved in the fabrication of the MEA are the same as those described above. The anodic EC layer of the MEA comprises the HiSPEC™ 4000Pt/C EC with a Pt loading of 0.05 mg•cm$^{-2}$. The cathodic EC layer of the MEA comprises the $PtX_n$-CN/Gr EC with a Pt loading of 0.1 mg•cm$^{-2}$; the details of ink formulation and deposition were not specifically optimized for the $PtX_n$-CN/Gr EC for the sake of simplicity and to improve the comparability and the internal consistency of the LCA results.

Both MEAs are conditioned and tested as described in the following. The MEA is fed with 800 sccm of pure $H_2$ at the anode and 1700 sccm of air at the cathode. Both feeds are fully hydrated. The temperature is brought to 85 °C and the back pressure of the feeds is brought to 65 psi as the MEA is run in potentiostatic conditions. Each potentiostatic step lasts 5 min; the steps are carried out at the following cell potentials: 0.6 V; 0.4 V; 0.6 V; 0.8 V; and 0.2 V before starting again a new cycle of steps at 0.6 V. The potentiostatic cycling described above is carried out as long as the currents stabilize. Subsequently, the cathode is fed with 500 sccm of pure $O_2$; the potentiostatic cycling described above is carried out as long as the currents stabilize. Once the MEA is conditioned, the polarization curve of the MEA mounting at the cathode the GRM-enabled hierarchical $PtX_n$-CN/Gr EC is collected in the operating conditions described in the following. (i) Both feeds are fully hydrated and their pressure is equal to 5 bar; (ii) the anode is fed with 800 sccm of pure $H_2$, and the cathode is fed with 1700 sccm of air; and (iii) the temperature is set to 85 °C. The polarizion curve to the MEA mounting at the cathode the Pt/C EC is collected in the same operating conditions, with the only difference that the pressure is set to 2 bar.

## 3. Results and discussion

Section 3.1 reports the performance in operating conditions of the single PEMFC mounting as the cathode EC either the $PtX_n$-CN/Gr hierarchical EC or the conventional Pt/C reference EC. The MEA components, test conditions and performance figures are implemented in the modelling of the PEMFC stacks reported in Table 1. Section 3.2 displays and discusses the LCA results and uncertainties.

### 3.1. Performance of ECs in single PEMFC

The polarization curves of the PEMFCs comprising the MEAs described in Section 2.2, which mount at the cathode either the GRM-enabled hierarchical $PtX_n$-CN/Gr EC or the Pt/C EC are displayed in Fig. 2(a). The performance figures of the PEMFCs are determined at a cell voltage of 0.6 V, a condition similar to typical operating conditions in applications [21]. Such performance figures include: (i) the power density, expressed as W·cm$^{-2}$ and displayed in Fig. 2(b); and (ii) the specific power, expressed as kW·$g_{Pt}^{-1}$ and reported in Fig. 2(c). The specific power is determined normalizing the power density (expressed as W·cm$^{-2}$) on the total Pt loading on both electrodes of the MEA (anode + cathode, expressed as $mg_{Pt}$·cm$^{-2}$). The performance of the MEA mounting the $PtX_n$-CN/Gr EC at the cathode is improved in comparison to that of the MEA only mounting the conventional Pt/C reference EC if we consider current densities lower than *ca.* 1.4 A·cm$^{-2}$. Indeed, in these conditions, the cell voltage of the MEA mounting the $PtX_n$-CN/Gr EC at the cathode is higher by a few tens of mV in comparison with the cell voltage of the MEA only mounting the conventional Pt/C reference EC. This result is achieved even if the loading of Pt at the MEA cathode provided by the $PtX_n$-CN/Gr EC is only one third of the loading of Pt at the MEA cathode provided by the Pt/C reference EC (*i.e.*, 0.1 $mg_{Pt}$·cm$^{-2}$ *vs.* 0.3 $mg_{Pt}$·cm$^{-2}$). At current densities higher than *ca.* 1.4 A·cm$^{-2}$ the cell voltage of the MEA mounting the $PtX_n$-CN/Gr EC decreases below the level of the MEA only mounting the Pt/C reference EC. This is likely due to mass transport issues associated with the different morphology of $PtX_n$-CN/Gr EC in comparison with the Pt/C reference EC.

### 3.2. Life cycle impact assessment results

Table 4 reports the results of the life cycle impact assessment phase, while Fig. 3 displays the results of a contribution analysis of the different components. The *"I-stack"* resulted to exhibit an improved performance in comparison with the *"R-stack"* in most of the impact assessment categories, with the exception of: (i) *"ozone layer depletion"*; (ii) *"freshwater aquatic ecotoxicity"*; and (iii) *"terrestrial ecotoxicity"*. With respect to the *"R-stack"*, the potential environmental impact of the *"I-stack"* in most of the impact categories is significantly lower, with a reduction between 27 and 44 %. As for the impact categories *"renewable primary energy demand"* and *"ionizing radiation"* the reduction is not as high (5–7 %). Finally, for those impact categories for which the potential environmental impact of the *"I-stack"* is higher with respect to the *"R-stack"*, the difference is between 20 and 30 %.

## 4. Discussion

### 4.1. Contribution analysis

The EC and, to a lesser extent, the GDLs provided the largest contribution to the impact category *"global warming potential"* of the PEMFC stacks (see Fig. 2 of Supplementary Materials). In both instances the contribution is mainly due to the use of electricity, that is required for: (i) the primary platinum extraction (in the case of the ECs); and (ii) the fabrication process (in the case of the GDLs). A similar trend is observed for the impact categories *"abiotic depletion of fossil fuels"*, *"non-renewable energy demand"*, *"human toxicity"* and *"marine water ecotoxicity"*. In both cases, the relative contribution on the impact category caused by the ECs and the GDLs is equal to *ca.* 80 % and *ca.* 10 %, respectively. The ECs provide the highest contribution in the impact categories *"acidification"*, *"eutrophication"*, *"abiotic depletion of elements"*, *"photochemical ozone formation"*, *"particulate matter"* and *"land*

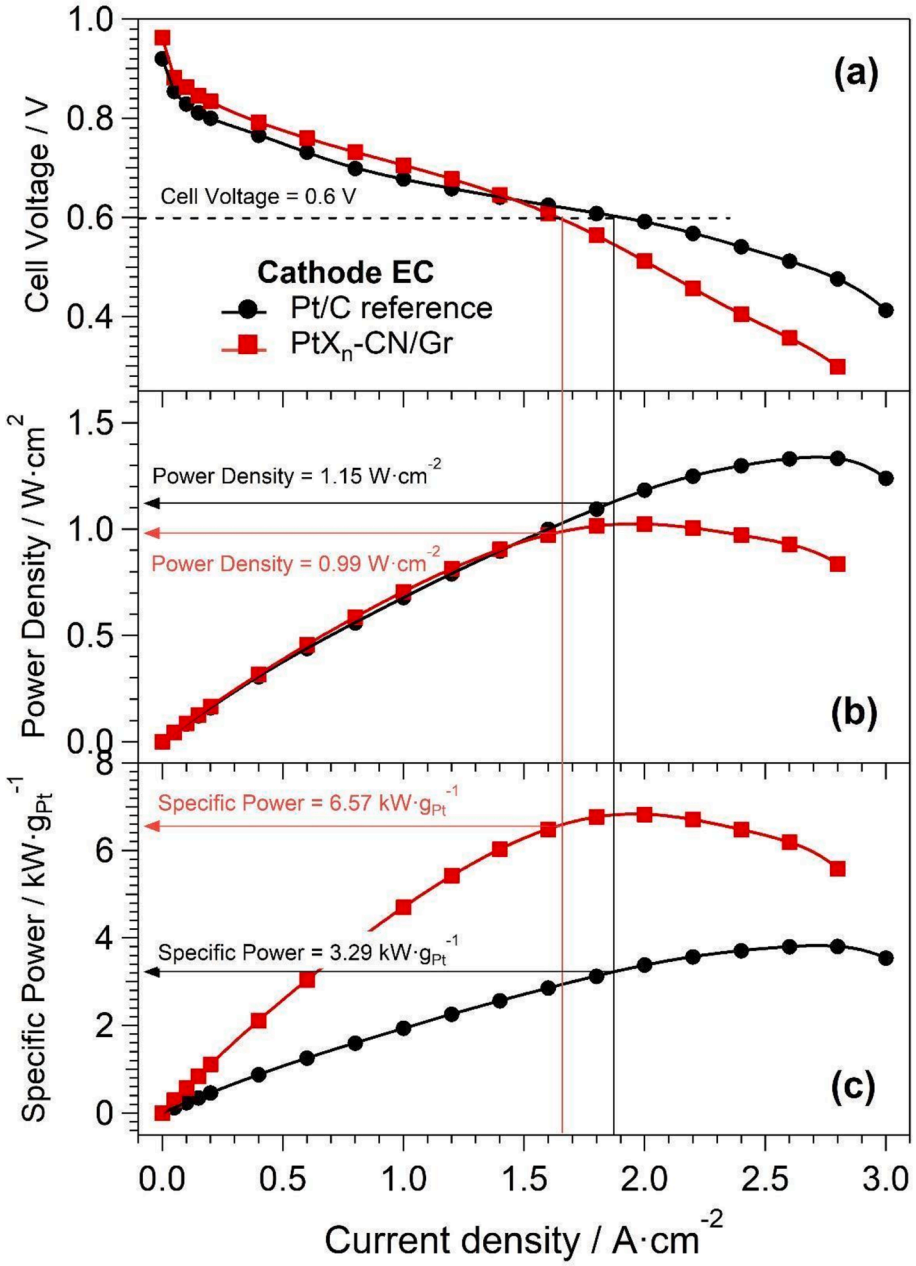


**Fig. 2.** Polarization curves (a); power density (b); and specific power (c) of the PEMFCs comprising the MEAs mounting at the cathode either: (i) the Pt/C reference EC; and (ii) the $PtX_n$-CN/Gr EC. The features of the MEAs and the test conditions are reported in Section 2.2.

*use"*, due to the life cycle of platinum including its mining and refinement. Regarding contributions associated to *"freshwater ecotoxicity"* and *"terrestrial ecotoxicity"* a high influence, despite electricity, is given by ethanol production related to $K_2PtCl_4$ synthesis. The impact category *"ozone layer depletion"* exhibits a different behavior, since it is mostly determined by the PEM and in particular by the Nafion ionomer therein. The *"I-stack"* includes more MEAs than the *"R-stack"* (304 + 57 *vs.* 261, see Table 1). Thus, with respect to the *"I-stack"*, the amount of Nafion ionomer included in the *"R-stack"* is lower, yielding a lower figure for the impact category *"ozone layer depletion"*. The impact categories *"ionizing radiation"* and *"renewable primary energy demand"* are correlated. Indeed, the *"ionizing radiation"* impact category is mainly ascribed to the fraction of nuclear energy present in the renewable energy mix used in the *"renewable primary energy demand"* impact category. The impact categories *"ionizing radiation"* and *"renewable primary energy demand"* are determined almost exclusively by the EC and the GDLs, which provide comparable relative contributions.

### 4.2. Uncertainty analysis

The results of the Monte Carlo analysis are displayed in Fig. 3. Results reveal that for more than 95 % of the runs the values of the impact categories of the *"I-stack"* are lower than those exhibited by the *"R-stack"*. The impact categories *"renewable primary energy demand"* and *"ionizing radiation"* are exceptions, though even in these two cases the *"I-stack"* offers an improvement over the *"R-stack"* for over 80 % of the runs. The Monte Carlo analysis also indicates that, with respect to the *"R-stack"*, the *"I-stack"* never yields a lower figure for the impact category *"ozone layer depletion"*. Based on this, in accordance with general assumptions [18,31], the improvement in the impact categories offered by the *"I-stack"* over the *"R-stack"* can be considered significant. The reliability of the results of this analysis is further assessed by the

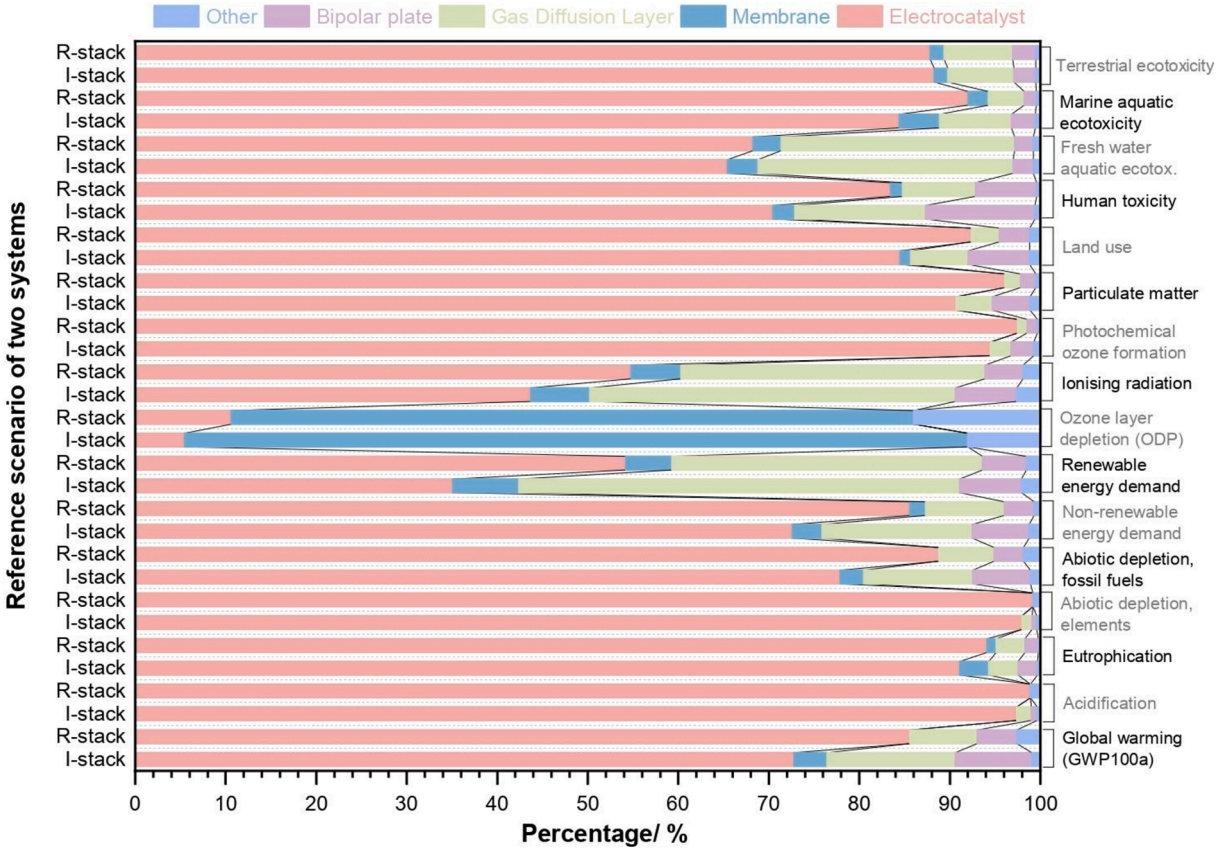


**Fig. 3.** Contribution analysis of components.

graphical representation of the uncertainty distribution of the values for each impact category. The corresponding boxplots are retrieved in Fig. 1 of Supplementary Materials.

Results reveal that for more than 95 % of the runs, the values of the impact categories of the *"I-stack"* are lower than those exhibited by the *"R-stack"*. The impact categories *"renewable primary energy demand"* and *"ionizing radiation"* are an exception, though even in these two cases the *"I-stack"* offers an improvement over the *"R-stack"* for more than 80 % of the runs. The Monte Carlo analysis also indicates that, with respect to the *"R-stack"*, the *"I-stack"* never yields a lower figure for the impact category *"ozone layer depletion"*. Based on these results, in accordance with general assumptions [18,31], the improvement in the impact

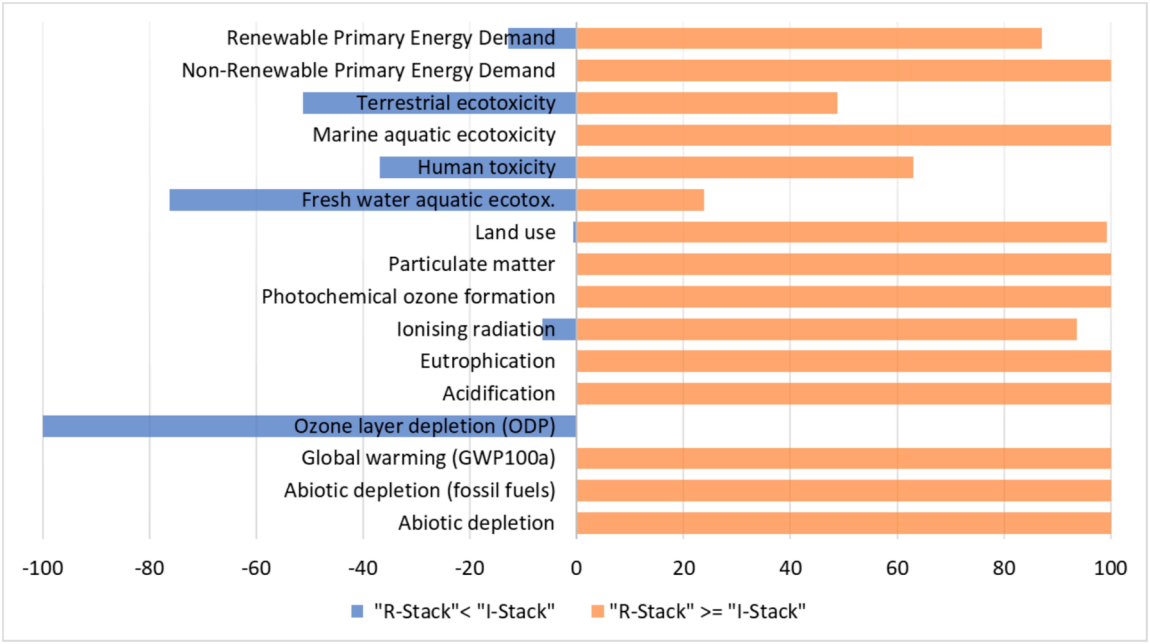


**Fig. 4.** Distribution of the results of Monte Carlo analysis after 1000 iterations.

categories offered by the *"I-stack"* over the *"R-stack"* can be considered significant for most of the impact categories considered here. This cannot be concluded for *"renewable primary energy demand"*, *"terrestrial ecotoxicity"*, *"human toxicity"*,*"freshwater ecotoxicity"* and *"ionizing radiation"*. The reliability of the results of this analysis is further assessed by the graphical representation of the uncertainty distribution of the values for each impact category. The corresponding boxplots are retrieved in Fig. S1 of Supplementary Materials (Fig. 4).

### 4.3. Sensitivity analysis

Fig. 5 reports on the results of the sensitivity analysis.

In the Sensitivity 1, where 60 % of the platinum used in the synthesis of the ECs is obtained from end-of-life recovery of automotive catalytic converters, it is observed that: (i) in general, the potential environmental impact is significantly decreased; and (ii) the ECs continue to provide the largest contribution to most impact categories. Similarly with the base case scenario, the exceptions are the following impact categories: (i) *"ozone layer depletion"*, where the largest contribution is still provided by the PEM; and (ii) *"ionizing radiation"* and *"energy demand, renewable"*, where the GDLs play a prominent role. The model resulted to be sensitive to this assumption. Considering the evolution of the market towards a more significant use or recycled Pt, the results of the base case scenario resulted to be conservative and confirmed. *"I-stack"*, when compared to the *"R-stack"*, presents lower potential environmental impacts in most of the impact categories investigated.

In Sensitivity 2, the Nafion proton-exchange ionomer is modeled in accordance with a less conservative approach [48] if compared to the one adopted in the base case [39]. Results show that impact assessment results are not sensitive to the modelling of Nafion apart from for the impact category *"ozone layer depletion"*. It must be noted that no data on the categories Non-Renewable, TOTAL and Renewable, TOTAL are not

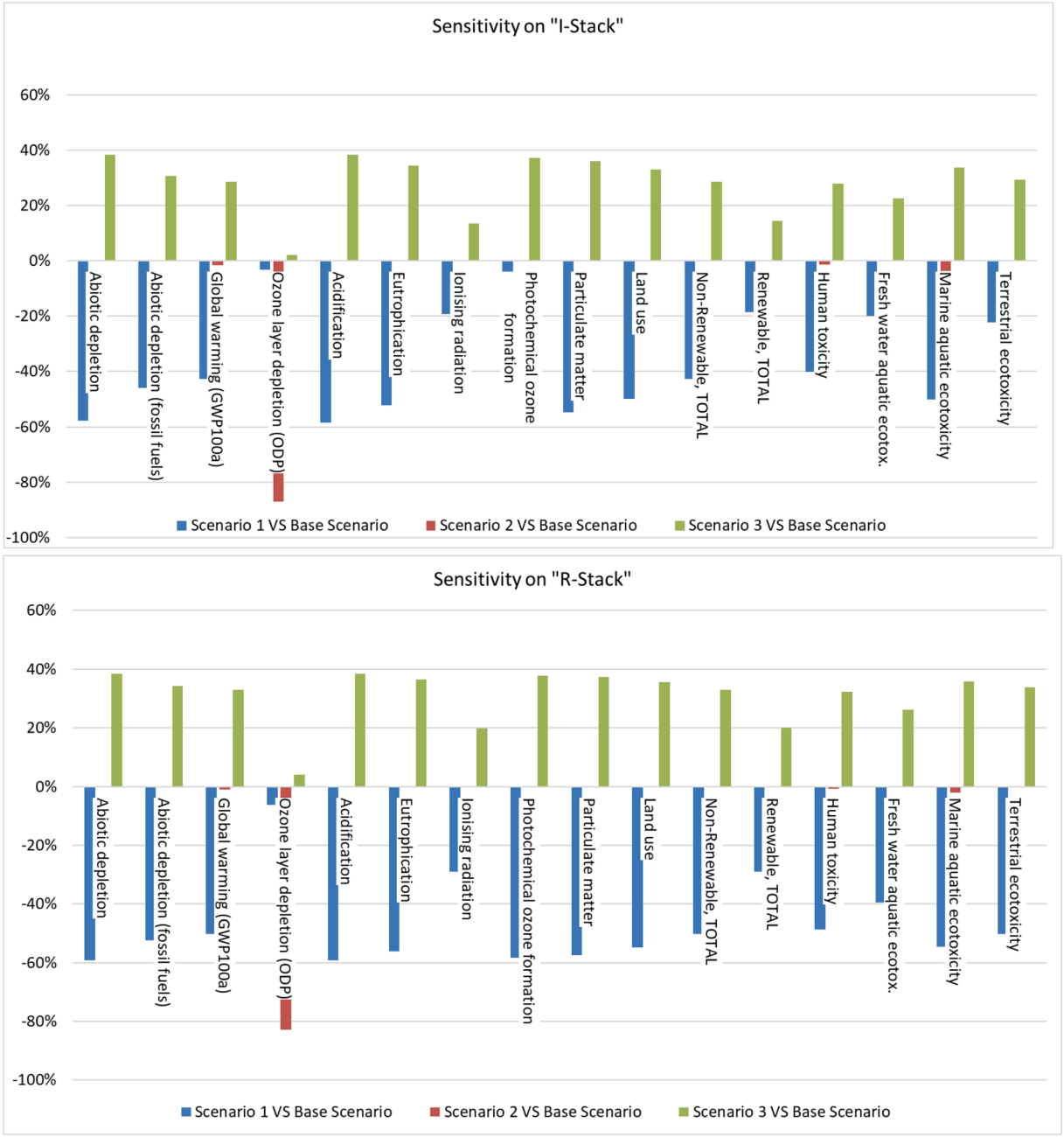


**Fig. 5.** Sensitivity analysis results.

available in the literature, therefore nothing can be concluded on these. Further investigations are needed to determine such impacts and will be the subject of future studies.

Finally, in scenario number 3, different efficiencies in the production of ECs are investigated by comparing industrial production (base case) with laboratory scale production. In the latter the potential environmental impacts increase by up to *ca.* 25 %. This is mainly due to the higher losses of EC and of the platinum therein triggered by (see Table 3): (i) the lower efficiency in EC production; and (ii) the lack of platinum recycling. As for Sensitivity 1, the results of the base case scenario the life cycle model resulted to be sensitive to this assumption and results of the impact assessment are confirmed. *"I-stack"*, when compared to the *"R-stack"*, presents lower potential environmental impacts in most of the impact categories investigated.

### 4.4. Discussion with literature review results

It is highlighted that in the present study the system boundary is set at the construction of PEMFC cells; end-plates and fittings are neglected (see Section 2.1.1). Accordingly, the comparison between the results obtained in this study and the literature is limited to the various components of the PEMFC stacks taken on their own. In the base case solution, the *"global warming potential"* for the ECs considered in the *"I-stack"* and in the *"R-stack"* is equal to 9.09 kg $CO_2$-eq/kW and 14.7 kg $CO_2$-eq/kW, respectively. These results are consistent with the literature, where values of 9 kg $CO_2$-eq/kW [24] and 14.6 kg $CO_2$-eq/kW [16] are reported. It is noted that both in the base case solution described in this study and in the literature, it is assumed that all platinum is obtained from primary sources. In the base case solution reported in this study, the modelling of the PEM (*i.e.*, a 14 μm Nafion reinforced by ePTFE) yields a value for the *"ozone layer depletion"* impact category equal to 7.13E-6 kg $CFC^{-11}$-eq/kW and 5.56E-6 kg $CFC^{-11}$-eq/kW for the *"I-stack"* stack and in the *"R-stack"*, respectively. These values are comparable with the figures reported in the literature, that fall in the range between 6.9 and 9.95E-6 kg $CFC^{-11}$-eq/kW [16] for a similar PEM exhibiting a thickness of 10 μm. Finally, in the base case solution the *"global warming potential"* for the GDLs considered in the *"I-stack"* stack and in the *"R-stack"* is equal to 1.77 kg $CO_2$-eq/kW and 1.28 kg $CO_2$-eq/kW, respectively. These values are similar to those reported in the literature [51], that reports a *"global warming potential"* for GDLs equal to 1.45 kg $CO_2$-eq/kW. In conclusion, the robustness of the LCA carried out in this work is supported by the fact that its outcomes are fully consistent with the results yielded by other studies reported elsewhere.

The recycling process efficiency was assumed to be 94 %, which can be considered reasonable for an industrial scale. This assumption takes into account alternative recycling methods studied at a laboratory scale, which show efficiencies ranging from 78 % to 85 % for ion exchange resin separation and solvent extraction. These values are aligned with the work of other scientists such as L. Duclos *et al.* [52]. Additionally, efficiencies of up to 96 % have been reported for a carbon-based extraction process, as reported by T. Bauer *et al.* [53].

## 5. Conclusions

The potential environmental impact of two PEMFC stacks yielding the same output power and comprising different cathodic ECs is evaluated by the LCA methodology. The components, operating conditions and performance of the PEMFC stacks are modeled on the basis of experimental results obtained from single PEMFCs. It is shown that, with respect to the *"R-stack"* mounting conventional Pt/C ECs, the *"I-stack"* mounting at the cathode the GRM-enabled hierarchical $PtX_n$-CN/Gr EC scores lower impacts in most of the environmental impact categories investigated: *"abiotic depletion"*, *"global warming potential"*, *"acidification"*, *"eutrophication"*, *"non-renewable primary energy demand"*, *"photochemical ozone formation"*, *"particulate matter"*, *"land use"* and *"marine water ecotoxicity"*. In the case of the potential environmental impact categories *"renewable primary energy demand"*, *"terrestrial ecotoxicity"*, *"human toxicity"*, *"freshwater ecotoxicity"* and *"ionizing radiation"*, the advantage or disadvantage provided by the *"I-stack"*, may not be considered significant under general assumptions [18,31]. Finally, with respect to the *"R-stack"*, the score of the *"I-stack"* in the potential environmental impact category *"ozone layer depletion"* is higher.

Results were investigated based on the contributions provided by the components of the PEMFC stacks. The largest contribution to the potential environmental impact categories is typically provided by the ECs due to extraction and processing of Pt, especially in the case when it is of primary extraction. It is revealed that from the environmental viewpoint it is advantageous to devise a PEMFC stack capable to minimize the amount of platinum per unit output power. It is also shown that the implementation in a PEMFC stack of ORR ECs very different from conventional *"state-of-the-art"* Pt/C ECs such as the GRM-enabled hierarchical $PtX_n$-CN/Gr EC can provide a major environmental advantage. This is true despite the peculiar features of the *"I-stack"* and of the GRM-enabled hierarchical $PtX_n$-CN/Gr EC therein, including: (i) the adoption of non-conventional reactants in the synthesis of $PtX_n$-CN/Gr such as GRMs; (ii) the necessity to carry out energy-intensive high-T treatments and post-processing steps during the synthesis of $PtX_n$-CN/Gr; (iii) the operation at a higher pressure in comparison with conventional Pt/C EC; and (iv) the slightly lower geometric power density registered in comparison with the *"R-stack"*. It is also highlighted that points (iii) and (iv) trigger an increase in the number of MEAs included in the PEMFC stack. Correspondingly, the mass of proton-exchange Nafion ionomer necessary for the PEMs and the EC layers in the *"I-stack"* is larger than that required by the *"R-stack"* modeled in this work. As a result, a higher score is registered for the *"I-stack"* in the potential environmental impact category *"ozone layer depletion"*, that is heavy influenced by the adoption of functional components comprising large amounts of halides (*e.g.*, Nafion, a perfluorinated macromolecule).

In summary, the development of advanced ORR ECs able to minimize the overall amount of platinum per unit output power is a very promising avenue to minimize the potential environmental impact of PEMFC stacks and, in perspective, of the entire PEMFC power plants that are implemented in vehicles and other embodiments of the *"hydrogen economy"*. The minimization of platinum loading has such a large impact that a broad variety of solutions for EC synthesis and PEMFC operation can be pursued meaningfully. The only significant drawback to be accepted is that in some instances it might be necessary to accept a higher score in the potential environmental impact category *"ozone layer depletion"*. In the same line, the sensitivity analysis presented in this work reveals that another highly promising strategy to minimize the potential environmental impact of the PEMFC technology is to maximize the amount of platinum obtained from recycling (*e.g.*, from a proper end-of-life waste management). This information could guide the rational development of the entire value chain of PEMFCs, with the purpose to further foster the large-scale implementation of the *"hydrogen economy"*.

## CRediT authorship contribution statement

**Giovanna Paladin:** Writing – original draft, Software, Investigation, Formal analysis, Data curation, Conceptualization. **Alessandro Manzardo:** Writing – review & editing, Validation, Supervision, Methodology, Conceptualization. **Angeloclaudio Nale:** Formal analysis, Data curation. **Enrico Negro:** Writing – review & editing, Validation, Supervision, Methodology, Formal analysis, Data curation, Conceptualization, Funding acquisition. **Vito Di Noto:** Writing – review & editing, Supervision, Resources, Project administration, Funding acquisition, Conceptualization.

## Declaration of competing interest

The authors declare that they have no known competing financial interests or personal relationships that could have appeared to influence

the work reported in this paper.

## Acknowledgments

This work was supported by the funds received in the framework of the following projects: (i) Graphene Flagship CORE 3; (ii) the project *"Advanced Low-Platinum hierarchical Electrocatalysts for low-T fuel cells"* funded by EIT Raw Materials; (iii) the project PERMANENT financed in the framework of the National Recovery and Resilience Plan (NRRP), M2C2, Investment Line 3.5; and (iv) the NRRP, M4C2 Investment 1.4 – Call for tender No. 3138 of December 16, 2021 of the Italian Ministry of University and Research – NextGenerationEU [Award Number: CNMS named MOST, Concession Decree No. 1033 of June 17, 2022, adopted by the Italian Ministry of University and Research, Spoke 14 *"Hydrogen and New Fuels"*].

## Appendix A. Supplementary data

Supplementary data to this article can be found online at https://doi.org/10.1016/j.cej.2025.159251.

## Data availability

Data will be made available on request.

## References

[1] E. Commission, COM(2019) 640 final - The European Green Deal, Bruxelles, 2019.
[2] E. Commission, COM(2020) 789 final - Sustainable and Smart Mobility Strategy – putting European transport on track for the future, Bruxelles, 2020.
[3] M.A. Aminudin, S.K. Kamarudin, B.H. Lim, E.H. Majilan, M.S. Masdar, N. Shaari, An overview: current progress on hydrogen fuel cell vehicles, Int. J. Hydrogen Energy 48 (11) (2023) 4371–4388, https://doi.org/10.1016/j.ijhydene.2022.10.156.
[4] M. Chourashiya, R. Sharma, S. Gyergyek, S.M. Andersen, Gram-size Pt/C catalyst synthesized using Pt compound directly recovered from an end-of-life PEM fuel cell stack, Mater. Chem. Phys. 276 (2022) 125439, https://doi.org/10.1016/j.matchemphys.2021.125439.
[5] E. Commission, E. for Internal Market Industry, Smes, M. Grohol, C. Veeh, Study on the critical raw materials for the EU 2023 – Final report, Publications Office of the European Union2023. doi: doi/10.2873/725585.
[6] X. Ren, Y. Wang, A. Liu, Z. Zhang, Q. Lv, B. Liu, Current progress and performance improvement of Pt/C catalysts for fuel cells, J. Mater. Chem. A 8 (46) (2020) 24284–24306, https://doi.org/10.1039/D0TA08312G.
[7] Y. Shao, G. Yin, Y. Gao, Understanding and approaches for the durability issues of Pt-based catalysts for PEM fuel cell, J. Power Sources 171 (2) (2007) 558–566, https://doi.org/10.1016/j.jpowsour.2007.07.004.
[8] V. Di Noto, E. Negro, B. Patil, F. Lorandi, S. Boudjelida, Y.H. Bang, K. Vezzù, G. Pagot, L. Crociani, A. Nale, Hierarchical metal–[carbon nitride "shell"/carbon "core"] electrocatalysts: a promising new general approach to tackle the ORR bottleneck in low-temperature fuel cells, ACS Catal. 12 (19) (2022) 12291–12301, https://doi.org/10.1021/acscatal.2c03723.
[9] V. Di Noto, E. Negro, K. Vezzù, F. Bertasi, G. Nawn, L. Toncelli, S. Zeggio, F. Bassetto, Electrocatalysts on carbonitride matrices, patent WO2017055981, 2017.
[10] L. Toncelli, S. Zeggio, F. Bassetto, M. Casarin, V. Di Noto, E. Negro, A. Nale, Y.H. Bang, K. Vezzù, G. Pagot, Method and plant for activating catalysts, patent WO2021064662, 2021.
[11] F. Lorandi, K. Vezzù, A. Nale, G. Pagot, Y.H. Bang, E. Negro, V. Di Noto, Tuning synthesis parameters and support composition for high-performing and durable core-shell Pt–Ni carbon nitride electrocatalysts for the oxygen reduction reaction, J. Power Sources 555 (2023) 232390, https://doi.org/10.1016/j.jpowsour.2022.232390.
[12] E. Negro, A. Nale, K. Vezzù, G. Pagot, S. Polizzi, R. Bertoncello, A. Ansaldo, M. Prato, F. Bonaccorso, I.A. Rutkowska, P.J. Kulesza, V. Di Noto, Hierarchical oxygen reduction reaction electrocatalysts based on FeSn0.5 species embedded in carbon nitride-graphene based supports, Electrochim. Acta 280 (2018) 149–162, https://doi.org/10.1016/j.electacta.2018.05.126.
[13] G. Flagship, Graphene Flagship, 2024. https://graphene-flagship.eu/. (Accessed 17 December 2024).
[14] V. Di Noto, E. Negro, S. Lavina, G. Pace, Electrocatalysts based on mono/plurimetallic carbon nitrides for polymer electrolyte membrane fuel cells fuelled with hydrogen (pemfc) and methanol (dmfc) and for hydrogen electrogenerators, patent WO2007119260A3, 2007.
[15] V. Di Noto, E. Negro, Core-shell mono/plurimetallic carbon nitride based electrocatalysts for low-temperaure fuel cells (pemfcs, dmfcs, afcs and electrolysers), patent WO2009157033, 2009.
[16] L. Usai, C.R. Hung, F. Vásquez, M. Windsheimer, O.S. Burheim, A.H. Strømman, Life cycle assessment of fuel cell systems for light duty vehicles, current state-of-the-art and future impacts, J. Clean. Prod. 280 (2021) 125086, https://doi.org/10.1016/j.jclepro.2020.125086.
[17] C. Corporation, Electrocatalyst for fuel cell electric vehicles, 2024. https://cataler.com/products/fcev/. (Accessed 18 December 2024).
[18] P. Masoni, A. Zamagni, Guidance Document for performing LCAs on Fuel Cells and $H_2$ Technologies, URL: https://www.hytechcycling.eu/wp-content/uploads/FC-Guidance-Document.pdf, 2011.
[19] H.A. Gasteiger, S.S. Kocha, B. Sompalli, F.T. Wagner, Activity benchmarks and requirements for Pt, Pt-alloy, and non-Pt oxygen reduction catalysts for PEMFCs, Appl. Catal. B 56 (1–2) (2005) 9–35, https://doi.org/10.1016/j.apcatb.2004.06.021.
[20] B.D. James, J.M. Huya-Kouadio, C. Houchins, D.A. Desantis, Mass Production Cost Estimation of Direct H 2 PEM Fuel Cell Systems for Transportation Applications: 2018 Update, 2018.
[21] G. Tsotridis, A. Pilenga, G. De Marco, T. Malkow, EU HARMONISED TEST PROTOCOLS FOR PEMFC MEA TESTING IN SINGLE CELL CONFIGURATION FOR AUTOMOTIVE APPLICATIONS, (2015). doi: 10.2790/54653.
[22] D.A. Cullen, K.C. Neyerlin, R.K. Ahluwalia, R. Mukundan, K.L. More, R.L. Borup, A. Z. Weber, D.J. Myers, A. Kusoglu, New roads and challenges for fuel cells in heavy-duty transportation, Nat. Energy 6 (5) (2021) 462–474, https://doi.org/10.1038/s41560-021-00775-z.
[23] R. Hischier, Life cycle assessment of engineered nanomaterials, Health and Environmental Safety of Nanomaterials, Elsevier 2021, pp. 443-458. doi: 10.1016/B978-0-12-820505-1.00001-8.
[24] S. Evangelisti, C. Tagliaferri, D.J.L. Brett, P. Lettieri, Life cycle assessment of a polymer electrolyte membrane fuel cell system for passenger vehicles, J. Clean. Prod. 142 (2017) 4339–4355, https://doi.org/10.1016/j.jclepro.2016.11.159.
[25] M. Grouchko, A. Kamyshny, K. Ben-Ami, S. Magdassi, Synthesis of copper nanoparticles catalyzed by pre-formed silver nanoparticles, J. Nanopart. Res. 11 (3) (2009) 713–716, https://doi.org/10.1007/s11051-007-9324-5.
[26] L. Duclos, M. Lupsea, G. Mandil, L. Svecova, P.-X. Thivel, V. Laforest, Environmental assessment of proton exchange membrane fuel cell platinum catalyst recycling, J. Clean. Prod. 142 (2017) 2618–2628, https://doi.org/10.1016/j.jclepro.2016.10.197.
[27] T.M. Gulotta, R. Salomone, F. Lanuzza, G. Saija, G. Mondello, G. Ioppolo, Life Cycle Assessment and Life Cycle Costing of unitized regenerative fuel cell: a systematic review, Environ. Impact Assess. Rev. 92 (2022) 106698, https://doi.org/10.1016/j.eiar.2021.106698.
[28] I. Kawano, Method for producing potassium tetrachloroplatinate, patent JP2820289B2, 1989.
[29] E.J. Iverson, D.M. Pierpont, M.A. Yandrasits, S.J. Hamrock, S.J. Obradovich, D.G. Peterson, Fuel cel subassemblies incorporating subgasketed thrifted membranes, patent US20110151350A1, 2014.
[30] S.C. Ball, G.A. Hards, M. Rodlert, J.D.B. Sharman, M.E. Spahr, Carbon supported catalyst, patent US9548500B2, 2017.
[31] F. Piccinno, R. Hischier, S. Seeger, C. Som, From laboratory to industrial scale: a scale-up framework for chemical processes in life cycle assessment studies, J. Clean. Prod. 135 (2016) 1085–1097, https://doi.org/10.1016/j.jclepro.2016.06.164.
[32] G. Geisler, T.B. Hofstetter, K. Hungerbühler, Production of fine and speciality chemicals: procedure for the estimation of LCIs, Int. J. Life Cycle Assess. 9 (2) (2004) 101–113, https://doi.org/10.1007/BF02978569.
[33] A.G. Parvatker, M.J. Eckelman, Comparative evaluation of chemical life cycle inventory generation methods and implications for life cycle assessment results, ACS Sustain. Chem. Eng. 7 (1) (2019) 350–367, https://doi.org/10.1021/acssuschemeng.8b03656.
[34] N. Tsoy, B. Steubing, C. van der Giesen, J. Guinée, Upscaling methods used in ex ante life cycle assessment of emerging technologies: a review, Int. J. Life Cycle Assess. 25 (9) (2020) 1680–1692, https://doi.org/10.1007/s11367-020-01796-8.
[35] V. Singh, D. Joung, L. Zhai, S. Das, S.I. Khondaker, S. Seal, Graphene based materials: past, present and future, Prog. Mater Sci. 56 (8) (2011) 1178–1271, https://doi.org/10.1016/j.pmatsci.2011.03.003.
[36] N. Kumar, R. Salehiyan, V. Chauke, O. Joseph Botlhoko, K. Setshedi, M. Scriba, M. Masukume, S. Sinha Ray, Top-down synthesis of graphene: a comprehensive review, FlatChem 27 (2021) 100224, https://doi.org/10.1016/j.flatc.2021.100224.
[37] S. Aktaş, B.N. ÇETİNER, Platinum recovery method, patent WO2021045709A1, 2020.
[38] W.C. Fernelius, Inorganic Syntheses, Volume II, Wiley, New York, 1946.
[39] A. Simons, C. Bauer, A life-cycle perspective on automotive fuel cells, Appl. Energy 157 (2015) 884–896, https://doi.org/10.1016/j.apenergy.2015.02.049.
[40] T.T. Ngo, T.L. Yu, H.-L. Lin, Nafion-based membrane electrode assemblies prepared from catalyst inks containing alcohol/water solvent mixtures, J. Power Sources 238 (2013) 1–10, https://doi.org/10.1016/j.jpowsour.2013.03.055.
[41] SimaPro 9.4.0.2., PRé Sustainability B.V., 2022.
[42] J. Committee for Guides in Metrology, First edition 2008 Evaluation of measurement data-Supplement 1 to the "Guide to the expression of uncertainty in measurement"-Propagation of distributions using a Monte Carlo method Évaluation des données de mesure-Supplément 1 du "Guide pour l'expression de l'incertitude de mesure"-Propagation de distributions par une méthode de Monte Carlo, 2008.
[43] Sfa, Heraeus, The Platinum Standard 2023 Produced in collaboration with Platinum crucibles for use in laboratory applications, Germany, 2023.
[44] A.E. Hughes, N. Haque, S.A. Northey, S. Giddey, Platinum group metals: a review of resources, production and usage with a focus on catalysts, Resources 10 (9) (2021) 93, https://doi.org/10.3390/resources10090093.

[45] E. Alonso, F.R. Field, R.E. Kirchain, Platinum availability for future automotive technologies, Environ. Sci. Technol. 46 (23) (2012) 12986–12993, https://doi.org/10.1021/es301110e.
[46] S. Spathariotis, K.M. Sakkas, E. Polyzou, I. Yakoumis, Recycling of platinum group metals from energy storage devices: a techno-economical business plan analysis, Open Research Europe 2 (2022) 92, https://doi.org/10.12688/openreseurope.14866.1.
[47] H.B. Trinh, S. Kim, T. Son, J. Lee, Platinum recycling from fuel cell-spent electrocatalysts using oxidative leaching in HCl solution, Cleaner Eng. Technol. 18 (2024) 100709, https://doi.org/10.1016/j.clet.2023.100709.
[48] M. Mori, R. Stropnik, M. Sekavčnik, A. Lotrič, Criticality and life-cycle assessment of materials used in fuel-cell and hydrogen technologies, Sustainability 13 (6) (2021) 3565, https://doi.org/10.3390/su13063565.
[49] L.C.A.D.A.N. Global, Global LCA Data Access Network (GLAD), 2024.
[50] V. Di Noto, E. Negro, A. Bach Delpeuch, F. Bertasi, G. Pagot, K. Vezzù, Graphene and other 2D materials as layered “shells” supported on “core” nanoparticle carriers, patent WO2018122368, 2018.
[51] M. Miotti, J. Hofer, C. Bauer, Integrated environmental and economic assessment of current and future fuel cell vehicles, Int. J. Life Cycle Assess. 22 (1) (2017) 94–110, https://doi.org/10.1007/s11367-015-0986-4.
[52] L. Duclos, R. Chattot, L. Dubau, P.X. Thivel, G. Mandil, V. Laforest, M. Bolloli, R. Vincent, L. Svecova, Closing the loop: life cycle assessment and optimization of a PEMFC platinum-based catalyst recycling process, Green Chem. 22 (6) (2020) 1919–1933, https://doi.org/10.1039/c9gc03630j.
[53] T. Bauer, K. Singh, G. Mandil, L. Svecova, L. Dubau, Identification of the environmental hotspots of a recycling process - Case study of a Pt PEMFC catalyst closed-loop recycling system evaluated via life cycle assessment methodology, Int. J. Hydrogen Energy 63 (2024) 396–410, https://doi.org/10.1016/j.ijhydene.2024.03.023.